© 2016. Published by The Company of Biologists Ltd | Journal of Experimental Biology (2016) 219, 528-534 doi:10.1242/jeb.126854

RESEARCH ARTICLE

The role of human ankle plantar flexor muscle–tendon interaction and architecture in maximal vertical jumping examined *in vivo*

Dominic James Farris[1,2,*], Glen A. Lichtwark[1], Nicholas A. T. Brown[2] and Andrew G. Cresswell[1]

ABSTRACT

Humans utilise elastic tendons of lower limb muscles to store and return energy during walking, running and jumping. Anuran and insect species use skeletal structures and/or dynamics in conjunction with similarly compliant structures to amplify muscle power output during jumping. We sought to examine whether human jumpers use similar mechanisms to aid elastic energy usage in the plantar flexor muscles during maximal vertical jumping. Ten male athletes performed maximal vertical squat jumps. Three-dimensional motion capture and a musculoskeletal model were used to determine lower limb kinematics that were combined with ground reaction force data in an inverse dynamics analysis. B-mode ultrasound imaging of the lateral gastrocnemius (GAS) and soleus (SOL) muscles was used to measure muscle fascicle lengths and pennation angles during jumping. Our results highlighted that both GAS and SOL utilised stretch and recoil of their series elastic elements (SEEs) in a catapult-like fashion, which likely serves to maximise ankle joint power. The resistance of supporting of body weight allowed initial stretch of both GAS and SOL SEEs. A proximal-to-distal sequence of joint moments and decreasing effective mechanical advantage early in the extension phase of the jumping movement were observed. This facilitated a further stretch of the SEE of the biarticular GAS and delayed recoil of the SOL SEE. However, effective mechanical advantage did not increase late in the jump to aid recoil of elastic tissues.

KEY WORDS: Biomechanics, Ultrasound, Fascicle, Elastic, Moment arm

INTRODUCTION

Maximal jumping requires large power outputs. This is because increasing limb force for a maximal effort reduces the time in contact with the ground and, thus, the time available for muscles to do work. In fact, power output during jumping can exceed what muscle contractile elements are capable of (Roberts and Azizi, 2011) and has been termed 'supramaximal' power output. The mechanisms that facilitate such 'power amplification' have been studied in detail in animals. In particular, insect and anuran species that exhibit exceptional jumping performance have received attention (Bennet-Clark, 1975; Alexander and Bennet-Clark, 1977; Roberts and Marsh, 2003; Astley and Roberts, 2012). Central to their ability to generate supramaximal power is the use of elastic elements to store and return energy in a catapult-like fashion (Roberts and Azizi, 2011). In vertebrates, this catapult mechanism involves the contractile elements doing work slowly to stretch series elastic elements (SEEs) prior to the onset of movement, and the SEEs subsequently recoil at high velocity to produce rapid movement and do work on the body at higher power outputs than could be achieved by the contractile elements alone. The fast recoil of the SEEs also permits slower shortening velocities of the contractile elements, enabling them to generate more force and do more positive work during shortening (Bobbert, 2001; Roberts and Azizi, 2011).

Some insects achieve slow storage of energy through physical catch mechanisms that impede joint movement as muscles generate tension. Subsequent release of the catch permits the necessary rapid recoil of elastic tissues (Alexander and Bennet-Clark, 1977). Anuran species have no physical catch mechanism, but it has been suggested that they vary the effective mechanical advantage (EMA) of hind limb muscles during limb extension to achieve a similar effect (Roberts and Marsh, 2003). This theory has recently been refined by Astley and Roberts (2014), who highlighted two mechanisms by which jumping frogs enhance the catapult-like storage and return of energy in distal hind limb tendons. Astley and Roberts (2014) observed: (1) EMA of ankle muscles was low early (to impede joint motion) and high late (to facilitate recoil) in the movement, and (2) large proximal joint (hip and knee) moments occur early in the movement, generating high ground reaction forces (GRFs) that provide resistance to ankle rotation and allow stretching of ankle SEEs. Combined, these mechanisms were redefined as a 'dynamic catch' that acts in addition to the resistance of body weight to help store and return elastic energy in tendons.

Like frogs, humans have no physical catches in their legs, but a catapult-like mechanism has been observed in muscle–tendon units (MTUs) of the human lower limb during walking and jumping (Hof et al., 1983; Kurokawa et al., 2001; Ishikawa et al., 2005; Lichtwark and Wilson, 2008). Most notable exponents are the muscles of the triceps-surae (gastrocnemius and soleus) that insert through the long-compliant Achilles tendon. These muscles are prime movers of the ankle joint, which is a key site of power release in jumping (Bobbert, 2001). Kurokawa et al. (2001) used ultrasound imaging of gastrocnemius muscle fascicles to show that substantial stretch and recoil of the gastrocnemius' SEE occurs during vertical squat jumping. These authors also estimated gastrocnemius (GAS) muscle and tendon power outputs to highlight a substantial contribution from the SEE to positive ankle power. Furthermore, simulations of human jumping show that recoil of elastic tissues increased ankle muscle force production and positive work (Bobbert, 2001) but it was not clear how the mechanics of the squat jump facilitated this catapult mechanism. Bobbert and van Ingen Schenau (1988) have previously observed a proximal-to-distal sequencing of joint moments in human jumping. However, it remains to be shown whether humans effectively employ the 'dynamic catch' mechanisms described by Astley and Roberts (2014). Furthermore, ankle power is generated by both the soleus

[1]School of Human Movement & Nutrition Sciences, The University of Queensland, Building 26B, Blair Drive, Brisbane, Queensland 4072, Australia. [2]Australian Institute of Sport, Bruce, ACT 2617, Australia.

*Author for correspondence (d.farris@uq.edu.au)

Received 17 June 2015; Accepted 29 November 2015

Journal of Experimental Biology

Journal of Experimental Biology (2016) 219, 528-534 doi:10.1242/jeb.126854

List of abbreviations

EMA	effective mechanical advantage
EMG	electromyography
GAS	gastrocnemius
GRF	ground reaction force
GRF_v	vertical ground reaction force
MTU	muscle–tendon unit
SEE	series elastic element
SOL	soleus

(SOL) and the GAS, which differ fundamentally in that the former is monoarticular and the latter biarticular. Consequently, the two muscles will be affected differently by the sequence of joint rotations and may exhibit different elastic mechanisms.

The purpose of this study was to compare *in vivo* measurements of human GAS and SOL MTU mechanics during maximal vertical squat jumping and determine the skeletal mechanics that facilitate these muscular actions. Based on data from human studies and anuran models, we predicted that a catapult mechanism would be present in both muscles that would be facilitated by: (1) gravitational loading of elastic tissues; (2) a proximal-to-distal sequence of joint moments; and (3) variable EMA (low-to-high). Furthermore, we predicted that the GAS length changes would be out of phase (delayed) compared with those of SOL because of knee extension counteracting ankle plantar flexion and allowing a prolonged stretch of this muscle and its series elastic tissues to aid in power production later in the take-off phase, when the tendon recoils.

MATERIALS & METHODS

Experimental protocol

Ten male athletes (mean±s.d. age=21±2 years, height=1.79±0.05 m, mass=84.8±7.1 kg) gave written informed consent to participate in this study that was approved by an institutional ethical review committee. Each participant completed three maximal vertical squat jumps starting from a squatted position (knees flexed to 90 deg, heels on the ground) that they held for 2 s before jumping. Participants were not specifically trained for jumping but were familiar with performing explosive jumping tasks.

Body mechanics

An eight-camera motion capture system (Oqus, Qualysis, Sweden) was used to record the three-dimensional positions of 37 reflective markers attached to the pelvis and lower limbs (modified Cleveland Clinic marker set). Twenty of the markers (calibration markers) were placed on strategic anatomical landmarks to define and scale the segments of a seven-segment rigid body model incorporating feet, shanks, thighs and pelvis. For the pelvis, markers were placed over the anterior superior iliac spines (left and right), posterior superior iliac spines (left and right) and the sacrum. The thighs had markers placed over the lateral and medial aspects of the knee joint line and functional joint centres were calculated for the hips. Shank calibration markers included the knee markers and markers placed over the lateral and medial malleoli. For the feet, markers were placed on participant's shoes over the first and fifth metatarsal–phalangeal joints, the calcaneus and the superior aspect of the most distal tip of the toes. The remaining markers were clusters of four markers attached to rigid plates and strapped to the thigh and shank segments that served to track the motion of these segments during jumping. Calibration markers on the feet and pelvis also served as tracking markers for these segments. Marker positions were sampled at 200 Hz and logged synchronously with other data via an analogue to digital convertor by Qualisys Track Manager software (Qualisys, Sweden). All marker position data were filtered with a second-order low-pass Butterworth digital filter using a cut-off frequency of 10 Hz.

The generic rigid body model used was that of Arnold et al. (2010), modified by removing all segments above the pelvis. The rigid body model was first scaled to the dimensions of each individual participant using static and dynamic calibration trials to create a scaled model of each participant. In the dynamic trial, the three-dimensional motion of the pelvis markers and the cluster of markers attached to the thigh were tracked as the participant performed several 'hula-hooping' type motions that exploited the full range of circumduction at the hip joints. These data were used to compute the location of a functional hip joint centre in the calibration trials, using Visual 3D software and its inbuilt algorithm based on the methods of Schwartz and Rozumalski (2005). In the static trial, the participants stood in a comfortable stance, as still as possible, whilst the positions of all markers were recorded. Marker positions and functional hip joint centre locations in the static trial were then used to scale the generic model segments to the dimensions of the participants. This scaling was based on pairs of calibration markers on each segment. A scale factor for each segment was calculated as the distance between two calibration markers on that segment on the participant divided by the distance between the same markers on the generic model. The dimensions of each segment in the scaled model were computed as the dimensions in the generic model multiplied by the scale factor. Segment masses were scaled to sum to the mass of the participant's lower body (59% total body mass) and keep the distribution of mass among segments the same as is in the generic model. The inertia tensor describing each segment's inertial properties was then updated for the new dimensions and mass. All scaling and subsequent rigid-body modelling procedures were performed in OpenSim software (Delp et al., 2007). The pairs of markers for each segment were: pelvis – right and left anterior-superior iliac spines; thigh – functional hip joint centre and lateral knee joint; shank – lateral knee joint and malleolus; and foot – calcaneus and tip of toes.

OpenSim software v3.0 was also used to perform an inverse kinematic analysis for each jumping trial (for details, see Delp et al., 2007). Briefly, this process performs a weighted least-squares fit of the model markers to the experimental marker positions to obtain the pose of the model at each point in time; from this, joint angles can be determined. We also combined the model kinematics with measured GRF data recorded from two force platforms (Bertec 4060-NC, one under each foot) in an inverse dynamics analysis to compute net muscle moments at the ankle, knee and hip joints using OpenSim v3.0. These moments were multiplied by joint velocities (the first derivative of joint angles) to obtain instantaneous joint powers for the ankle, knee and hip as per Farris and Sawicki (2012a). Joint angles are the internal angles between proximal and distal segments with positive changes/velocities indicating extension. Positive joint moments and powers represent moments acting to extend the joint and the rate of work being done to extend the joint.

MTU mechanics

The rigid body model included MTU paths for the GAS (medial and lateral heads) and SOL, allowing computation of MTU length and moment arm about joints for these muscles at each point in time. Muscle moment arms are hereafter also referred to as input muscle moment arms, as muscle forces are inputs to the system. The output

Journal of Experimental Biology (2016) 219, 528-534 doi:10.1242/jeb.126854

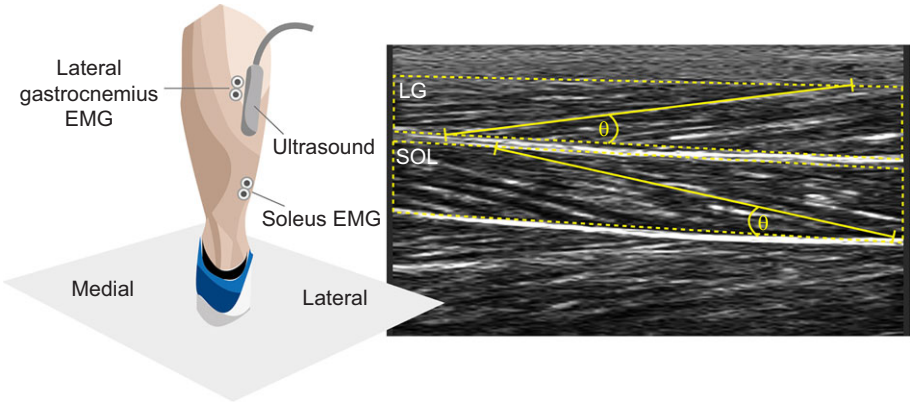

Fig. 1. The positioning of the ultrasound transducer and an example ultrasound image. The transducer was placed over the lateral head of the gastrocnemius such that both soleus and lateral gastrocnemius fascicles could be visualised throughout the thickness of each muscle. Yellow dashed lines outline sagittal cross-sections of the two muscles and the solid yellow lines are digitisations of fascicles within each muscle. LG, lateral gastrocnemius; SOL, soleus; θ, pennation angle.

was GRF and the moment arm of the GRF at the ankle joint is therefore referred to as the output GRF moment arm. EMA was defined as the ratio of the input moment arm to the output moment arm. Muscle fascicle lengths for the lateral GAS and SOL of the right leg were measured from dynamic ultrasound imaging of these muscles (Lichtwark and Wilson, 2006; Farris et al., 2013). A 96-element linear array ultrasound transducer (LZ 7.5/60/96Z, Telemed, Lithuania) was placed over the belly of GAS and at an orientation such that fascicles of both GAS and SOL could be visualised throughout the muscles (Fig. 1). A systematic review of validity and reliability of using 2D ultrasound images to measure fascicle length and pennation showed good reliability and validity of this technique (Kwah et al., 2013). The transducer was bandaged securely to the leg to hold it in place during the movement. Ultrasound images were sampled at 80 Hz and the length of GAS and SOL fascicles were measured in each image using a previously described tracking algorithm and procedures (Cronin et al., 2011). We assumed a Hill-type muscle arrangement and that the difference in length change between the fascicle and MTU was attributable to the SEE. To estimate the length of the SEE, we multiplied the length of the fascicle by the cosine of pennation angle (Fig. 1) and subtracted this from MTU length as per previously published methods (Lichtwark and Wilson, 2006; Farris and Sawicki, 2012b).

Electromyography

Surface electromyography (EMG) was used to measure muscle activation for the GAS and SOL of the right leg. A bipolar electrode configuration with a separation of ~20 mm was used and electrodes were placed over the belly of the respective muscles and aligned along the direction of the underlying muscle fascicles (placements highlighted in Fig. 1). Raw EMG signals were sampled at 2000 Hz synchronously with motion capture data and processed with a custom MATLAB (The MathWorks, Natick, MA, USA) algorithm. Raw signals had the DC offset removed and were then band-pass filtered (20–300 Hz), rectified and averaged with a rolling root-mean-squared calculation over consecutive windows of 100 ms.

Data reduction

All time series data were cropped to the movement phase between the onset of upward motion to the point of take-off. Onset of upward motion was identified as when the velocity of a marker attached over the sacrum exceeded 0.05 m s^{-1} and take-off as when the combined vertical GRF (GRF_v) dropped below 10 N. Time series data between onset and take-off were resampled over 101 evenly spaced time points and averaged across participants to give group means. All data are for the right leg only. Onset of movement at ankle and knee joints was determined as the point at which angular velocity exceeded 50 deg s^{-1} (0.87 rad s^{-1}). To test for a statistical difference in the timing of elastic recoil between GAS and SOL, a paired *t*-test was employed. To test the sequence of joint moments, timing of peak extension moment was compared between joints via a repeated-measures ANOVA.

RESULTS

Joint level mechanics showed a trend for proximal-to-distal sequencing with hip extension followed by knee extension and finally followed by ankle plantar flexion (Fig. 2A). Representative poses and GRF vectors are shown at pertinent stages of a jump in Fig. 3. There was a significant (F=14.9, P=0.0008) difference in timing of peak extension moments occurring in the order: hip–knee–ankle (Fig. 2E). Positive power peaked earlier for the hip and knee than for the ankle (Fig. 2E,G). SOL MTU length began shortening at the onset of ankle plantar flexion, slowly at first followed by a phase of more rapid shortening over the last 30% of the movement (Fig. 2B, Table 1). This was accompanied by a more constant, relatively slower shortening of the SOL fascicles throughout the movement (Fig. 2D), and SOL averaged EMG

Table 1. Mean (±s.e.m.) length change (Δ*L*) of gastrocnemius (GAS) and soleus (SOL) muscle–tendon unit (MTU) components relative to initial length at key time points during limb extension (negative values indicate shortening)

		GAS Δ*L* (mm)			SOL Δ*L* (mm)		
	Time (%)	MTU	Fascicle	SEE	MTU	Fascicle	SEE
Onset of knee extension	22±4.4	0.0±0.0	−1.1±0.3	1.1±0.3	0.0±0.0	−0.7±0.2	0.7±0.2
Onset of ankle extension	42±5	1.1±0.2	−2.5±0.7	3.7±0.8	0.0±0.0	−1.8±0.2	1.0±0.4
Onset of GAS MTU shortening	59±4	1.2±0.4	−3.9±0.8	5.3±1.0	−3.0±1.0	−2.9±0.4	−0.2±1.0
Max. GAS SEE length	71±5	0.4±0.7	−5.0±0.8	5.8±1.0	−6.8±1.3	−3.8±0.5	−2.7±2.0
Take-off	100±0	−20±1.6	−8.6±1.5	−12.3±2.5	−49±2.0	−7.7±1.0	−39.3±3.0

SEE, series elastic element.

Journal of Experimental Biology

Journal of Experimental Biology (2016) 219, 528-534 doi:10.1242/jeb.126854

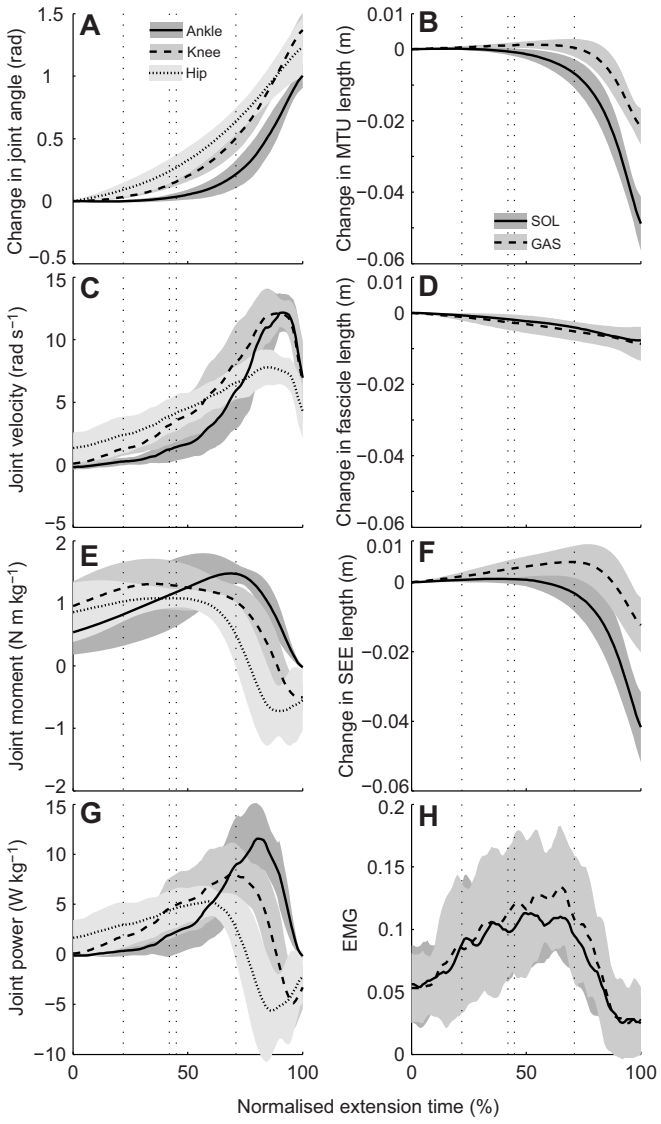

Fig. 2. Group mean (±s.d.) instantaneous joint and muscle mechanics plotted from the onset of upward motion through to take-off (time scale normalised to 101 points). (A) Change in joint angle; (B) change in muscle–tendon unit (MTU) length; (C) joint velocity; (D) change in fascicle length; (E) joint moment; (F) change in series elastic element (SEE) length; (G) joint power; (H) averaged electromyography (EMG) signal. The vertical dotted lines from left to right represent the timing of: onset of knee rotation, onset of ankle rotation, onset of SOL elastic recoil, and onset of GAS elastic recoil.

rising to a peak at approximately 70% of the way through limb extension before declining sharply to minimal levels in the last 30% of the movement (Fig. 2H). Calculations based on fascicle and MTU length changes of SOL estimated a pattern of SOL SEE length change that showed very small amounts of lengthening during the first 40% of the movement followed by a period (45–60%) of slow shortening and then a large amount of shortening late in the movement cycle (Fig. 2F, Table 1). SOL elastic recoil began at 45% of the way through limb extension.

Fascicle length change and averaged EMG exhibited similar trends for GAS as for SOL (Fig. 2D,H). The GAS MTU lengthened slowly from onset of motion until approximately 60% of the way through the movement (Fig. 2B, Table 1). Furthermore, the GAS SEE lengthened from onset until 71% of the way through the movement before shortening rapidly in the final third of the

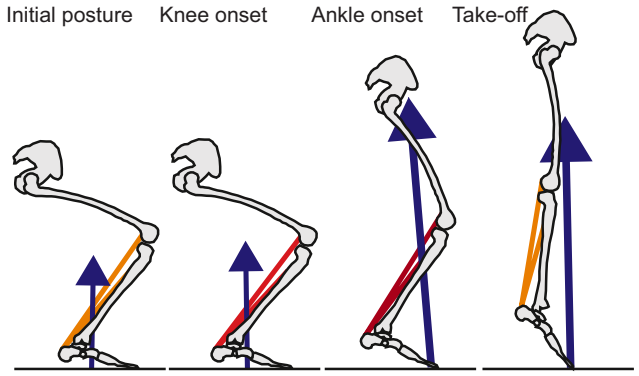

Fig. 3. Representative limb poses and ground reaction force (GRF) vector for one participant at key events in the jump motion. From left to right the pose is set to that: at initial posture, at the onset of knee rotation, at the onset of ankle rotation, and just prior to take-off. Blue arrows represent the GRF vectors and darker red colours of the muscles indicate greater muscle activation.

movement (Fig. 2F, Table 1). Onset of recoil for GAS occurred significantly (P=0.0002) later than for SOL. The MTU and fascicle velocities are shown in Fig. 4D and highlight the relatively slow and consistent fascicle shortening velocities compared with the large shortening velocities of the MTU that occurred in concert with elastic recoil (SEE shortening). GAS and SOL moment arms remained relatively constant for the first half of the movement before increasing in magnitude as the MTUs shortened and the SEE recoiled (Fig. 4A). The magnitude of the output GRF moment arm increased throughout the movement and was somewhat larger than the input muscle moment arms (Fig. 4A). As a result, SOL and GAS EMA initially decreased before plateauing from 70 to 90% of the movement and then decreased over the last 10% (Fig. 4C).

DISCUSSION

In this study we have observed through direct measurement that during a squat jump the human GAS and SOL exhibit stretch and recoil of their series elastic tissues in the catapult-like manner that has been associated with power amplification in muscle (Astley and Roberts, 2012). This is consistent with previous observations made in human medial GAS (Kurokawa et al., 2001) and simulations of plantar flexor mechanics during jumping (Bobbert et al., 1986; Anderson and Pandy, 1993). Previous work has considered the importance of plantar flexor SEE recoil in terms of its contribution to power output. Calculations suggested that recoil of the medial GAS SEE provides 4.4 J of the 5.1 J of positive work done by this muscle (Kurokawa et al., 2001), and that the plantar flexor SEEs contributed 70% of the total positive work of these muscles during squat jumping (Anderson and Pandy, 1993). Clearly, elastic recoil is crucial in these muscles and this highlights the need for mechanisms that facilitate it. The focus of this discussion will be the mechanisms that support elastic stretch and recoil in the plantar flexors during jumping.

Our hypotheses predicted that three mechanisms would exist to facilitate the observed elastic catapult action: (1) gravitational loading of plantar flexor series elastic tissues; (2) a proximal-to-distal sequence of joint moments; and (3) variable plantar flexor EMA shifting from low to high during leg extension. We also predicted that the biarticular nature of the GAS combined with the proximal-to-distal sequence of joint actions would prolong GAS SEE stretch and delay GAS SEE recoil compared with that of the SOL SEE. Evidence for each of these mechanisms will now be considered.

Journal of Experimental Biology (2016) 219, 528-534 doi:10.1242/jeb.126854

Gravitational loading and SEE stretch

A significant stretch of the SEEs prior to GRF_v exceeding one body weight would be evidence for gravitational loading contributing to storage of elastic energy. For a human squat jump, body weight is being supported in the initial posture, and GRF_v exceeds this value as soon as the upward motion begins (Fig. 4B). Therefore, significant stretch of the SEE in the initial posture would indicate an important contribution of gravitational loading to SEE stretch. We could not observe directly the lengthening of the SEE due to body weight support because there was no period prior to the initial posture when participants were not supporting body weight. However, observation of the lengthening and shortening that occurred during limb extension provided evidence.

The SOL and GAS SEEs recoiled by 39.3 and 12.3 mm, respectively (Table 1, Fig. 2F). However, from the onset of upward motion until the onset of SEE recoil, GAS SEE lengthened only by 5.8 mm and SOL SEE by 1.0 mm (Table 1, Fig. 2F). This meant that approximately half of the stretch of the GAS SEE and almost all of the stretch of the SOL SEE must have occurred prior to the onset of motion, in the initial posture. As can be seen from and Figs 1E and 3B, the net ankle moment was already at nearly half of its maximum value at the onset of limb extension. Furthermore, at the onset of limb extension the GAS and SOL were already at approximately half the peak activation achieved during the jump (Fig. 2H), indicating that they were actively producing force to contribute to this moment. Therefore, our data suggest that gravitational loading of plantar flexor SEEs is a major part of the mechanism for storing elastic energy in these tissues during human squat jumping.

The importance of body weight in storing elastic energy raises interesting comparisons to human countermovement jumping. Both Bobbert et al. (1996) and Anderson and Pandy (1993) concluded that recoil of elastic elements provided similar amounts of positive work in both countermovement and squat jumps. However, the mechanism of energy storage was different, with countermovement jumps using lost potential energy of the body as the source and squat jumps using muscle contractile work (Anderson and Pandy, 1993). The latter requires resistance to joint motion and here we have shown that a significant part of this resistance is due simply to body weight. Although participants lowered themselves into the squatted position, this was done slowly with a significant pause before jumping and a minimal change in ankle joint moment (5±6 Nm). Thus, we have presented further evidence that significant stretch of elastic tissues can be achieved in jumping without a countermovement. Alexander's (1995) simulations suggested that, for human-like levels of force production, a countermovement outperformed a squat jump when compliant SEEs are involved. However, in those simulations the squat jump was defined by extensors being inactive in the initial posture, which seems improbable.

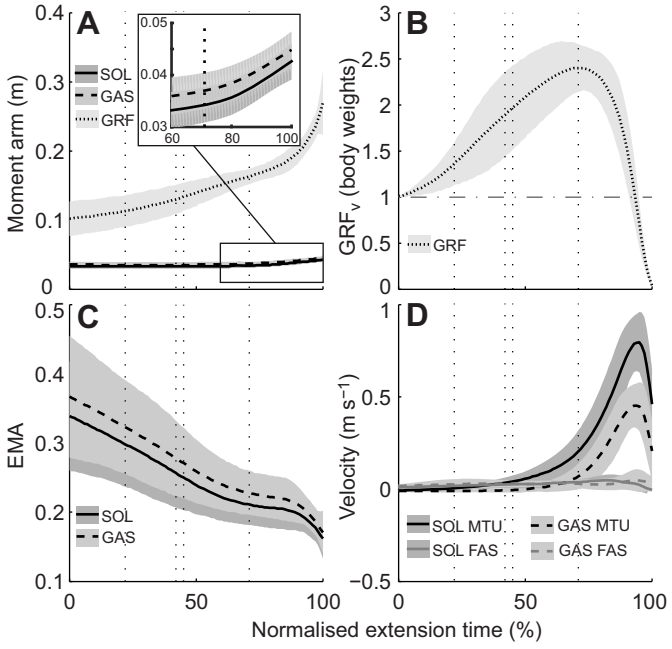

Fig. 4. Time series data for mechanical advantage, ground reaction force and MTU velocity. Group mean (±s.d.) (A) instantaneous moment arm, (B) vertical ground reaction force (GRF_v), (C) effective mechanical advantage (EMA) and (D) the velocities of the muscle–tendon units (MTUs) and fascicles. Data are plotted over 101 evenly spaced points between the onset of upward motion and take-off. The vertical dotted lines from left to right represent the timing of: onset of knee rotation, onset of ankle rotation, onset of SOL elastic recoil, and onset of GAS elastic recoil.

Joint kinetics and SEE stretch

There is evidence from human (Bobbert and van Ingen Schenau, 1988) and frog (Astley and Roberts, 2014) data that jumping performance is enhanced when ankle rotation, peak ankle moment and peak ankle power occur late during propulsion. Astley and Roberts (2014) proposed that a corresponding proximal-to-distal sequence of joint kinetics could aid energy storage and release in distal tendons. This was because the large early hip and knee muscle moments increase GRF above body weight as they accelerate proximal segments. This increase in GRF provides greater resistance to ankle joint rotation and, thus, ankle extensors were able to increase activation and muscle force so as to stretch their tendons and store energy. Our human data are in agreement with this result in frogs. In Fig. 2E it can be seen that hip and knee moments are greatest prior to the onset of ankle rotation. At the same time, GRF_v increased up to nearly two body weights (Fig. 4B), plantar flexor activation and moments increased and the GAS SEE was stretched (Fig. 2F). Therefore, our data are consistent with the hypothesis that increasing proximal joint moments early in the jump motion facilitates plantar flexor SEE stretch.

EMA and SEE mechanics

EMA was defined as the ratio of the length of the input muscle moment arm to the length of the output GRF moment arm. We hypothesised that at the start of the movement, plantar flexor EMA would be low. This was predicted because it would allow plantar flexors to generate more tension and stretch in the SEE, while minimising ankle rotation. However, at the beginning of the movement, the EMA of both SOL and GAS was actually at its greatest value (Fig. 4C) and EMA decreased throughout limb extension. This was largely because the output GRF moment arm progressively increased throughout limb extension (Fig. 4A). This finding was contrary to the hypothesis and opposite to the pattern of EMA previously observed for frog ankle muscle (Astley and Roberts, 2014). Therefore, it does not seem that humans incorporate variable EMA of plantar flexors as a 'catch-like' mechanism for enabling catapult action of plantar flexor SEEs during jumping.

Although the observed trend in EMA did not support a dynamic catch mechanism, it may have been appropriate for other reasons. In the initial posture, the jumper must support body weight. To minimise the effort required for this task, a high EMA is desirable. Thus, the initially higher EMA may have helped minimise ankle muscle forces required to support weight. Once the jumping motion is initiated, the need to store energy in plantar flexor SEEs becomes

Journal of Experimental Biology (2016) 219, 528-534 doi:10.1242/jeb.126854

important and can be aided by a low EMA. Therefore, the initial decrease in plantar flexor EMA after movement onset (Fig. 4C) would have assisted with this. However, the continued decrease in EMA following the onset of elastic recoil (Fig. 4C) was not appropriate for aiding rapid recoil of the SEEs. Carrier et al. (1994) observed trends in plantar flexor EMA during ground contact in running similar to those we observed for squat jumping (although their metric was gear ratio, the inverse of EMA). These authors proposed that increasing gear ratio (decreasing EMA) during stance would allow for plantar flexor shortening velocities that were better for active muscle fibre force and power production. Perhaps a similar benefit may be derived for jumping with the present observed trend in plantar flexor EMA, although MTU shortening is dominated by SEE recoil.

Biarticular GAS versus uniarticular SOL

There were distinct differences in the length changes of GAS and SOL during limb extension. Following the onset of ankle rotation, the muscle–tendon interaction in the biarticular GAS was distinctly different from that of the uniarticular SOL. The SOL MTU began to shorten at the onset of ankle rotation and continued to do so until take-off. Conversely, the GAS MTU slightly lengthened until approximately 60% of the way through the jump and did not start to shorten at a significant rate until well after SOL commenced shortening (Fig. 2B). This pattern of length change was facilitated by continued extension of the knee joint and relatively slower plantar flexion during this period (Fig. 2A,C). Previous analyses of human jumping showed that the GAS MTU shortens very slowly during this phase of the movement (Bobbert et al., 1986). The benefit of this was that GAS could act in a strut-like manner, transferring power generated by knee extensors to the ankle joint (Bobbert et al., 1986). Interestingly, our data show that the GAS is not just behaving like a strut during this time, but that the GAS SEE continued to stretch by a further 5.8 mm and GAS fascicles continued to shorten (Table 1, Fig. 2D,F). This is evidence that the GAS may not function simply to transport power from the knee to the ankle during this phase (as previously suggested), but may store some of the work done by knee extensors and GAS fascicles in its SEE for release later in the movement.

Potential limitations

Two-dimensional ultrasound imaging was used to visualise muscle fascicles that have been shown to have a three-dimensional curvature that may be hard to accurately image in any single plane (Rana et al., 2014). Despite this, a systematic review of the validity and reliability of two-dimensional ultrasound-based measures of muscle fascicle lengths showed good accuracy and reliability, although it is hard to test under dynamic conditions (Kwah et al., 2013). We did not compute muscle forces to complement SEE length data because of the inherent redundancy in computing muscle forces from joint moments. However, an approximation of GAS SEE stiffness can be made during the period when the GAS SEE lengthened and the SOL SEE did not, and we can assume that all of the increase in joint moment can be attributed to increasing GAS force. During this time, ankle joint moments increased by 0.8 Nm kg^{-1}. Using mean body mass (85 kg) and a typical GAS moment arm (0.05 m), this equates to an increase of GAS force of 1360 N. The lengthening of the GAS SEE was ~6 mm (Table 1) and thus stiffness was estimated as 233 N mm^{-1}. This is within the range of previously reported values for the GAS SEE (Lichtwark and Wilson, 2005). Furthermore, we represented the GAS and SOL SEEs as two separate SEEs even though they distally share a common tendon. The SEE of a muscle in our study is essentially a theoretical convenience that lumps together all tissues acting in series with the muscle, rather than a distinct physical entity. Therefore, one can consider that each muscle has an independent SEE even though a portion of it may be physically shared with another muscle.

As noted earlier, significant lengthening of the SOL SEE must have resulted from supporting body weight prior to movement when the ankle moment was less than half its peak value reached during the jump. Thus, the SOL SEE was stretched considerably more by the modest ankle moments observed in the squatted position than it was when the ankle moment doubled in magnitude during limb extension. This was rationalised above by attributing the increase in ankle moment to increases in GAS force. However, another factor might be that the force–length relationship of SEEs exhibits a J-shape, with a toe region at low forces where stiffness is lower and less energy is stored for a given increment in length. Thus, the large pre-stretch in the squatted position might be explained by the SOL SEE being in this toe region and the energy stored and made available for return may be less significant than initially assumed.

Conclusions

In this study we sought to examine *in vivo* muscle–tendon interaction in the biarticular GAS and uniarticular SOL muscles during maximal vertical squat jumping and identify mechanisms by which these muscles use elastic tissues to maximise power output. Our results highlighted that both muscles utilised significant stretch and recoil of their SEEs in a catapult-like fashion, which likely serves to maximise power output. Much of the stretch of plantar flexor SEEs appears to be generated against the resistance of gravitational loads in the initial squat posture. Further stretch of the GAS SEE and a delay of recoil in SOL was aided by large proximal joint moments and decreasing plantar flexor EMA early in the jumps. Stretch of the GAS SEE was further facilitated by its biarticular arrangement and extension of the knee joint. Rapid shortening velocities of the SOL and GAS MTUs were achieved by SEE recoil as it returned the previously stored energy to achieve high ankle power outputs, although this was not aided by any increase in plantar flexor EMA. Perhaps the inability of humans to manipulate EMA in a more favourable manner partially explains our modest jumping abilities compared with species more specialised for jumping, although recent data suggest that factors such as muscle contractile properties are also very important for jump performance (Plas et al., 2015).

Acknowledgements

We thank Mr Michael Erian for assisting with participant recruitment, data collection and analysis.

Competing interests

The authors declare no competing or financial interests.

Author contributions

All authors contributed to the conception and design of the study. D.J.F. conducted the data collection, performed data analysis and drafted the manuscript. G.A.L., A.G.C. and N.A.T.B. contributed to drafting of the manuscript. All authors gave final approval for publication.

Funding

D.J.F. is supported by a post-doctoral fellowship funded by the Australian Sports Commission.

References

Alexander, R. M. (1995). Leg design and jumping technique for humans, other vertebrates and insects. *Philos. Trans. R. Soc. B Biol. Sci.* **347**, 235-248.

Alexander, R. M. and Bennet-Clark, H. C. (1977). Storage of elastic strain energy in muscle and other tissues. *Nature* **265**, 114-117.

Anderson, F. C. and Pandy, M. G. (1993). Storage and utilization of elastic strain energy during jumping. *J. Biomech.* **26**, 1413-1427.
Arnold, E. M., Ward, S. R., Lieber, R. L. and Delp, S. L. (2010). A model of the lower limb for analysis of human movement. *Ann. Biomed. Eng.* **38**, 269-279.
Astley, H. C. and Roberts, T. J. (2012). Evidence for a vertebrate catapult: elastic energy storage in the plantaris tendon during frog jumping. *Biol. Lett.* **8**, 386-389.
Astley, H. C. and Roberts, T. J. (2014). The mechanics of elastic loading and recoil in anuran jumping. *J. Exp. Biol.* **217**, 4372-4378.
Bennet-Clark, H. C. (1975). Energetics of jump of locust *Schistocerca gregaria*. *J. Exp. Biol.* **63**, 53-83.
Bobbert, M. F. (2001). Dependence of human squat jump performance on the series elastic compliance of the triceps surae: a simulation study. *J. Exp. Biol.* **204**, 533-542.
Bobbert, M. F. and van Ingen Schenau, G. J. (1988). Coordination in vertical jumping. *J. Biomech.* **21**, 249-262.
Bobbert, M. F., Huijing, P. A. and van Ingen Schenau, G. J. (1986). An estimation of power output and work done by the human triceps surae muscle-tendon complex in jumping. *J. Biomech.* **19**, 899-906.
Bobbert, M. F., Gerritsen, K. G. M., Litjens, M. C. A. and Van Soest, A. J. (1996). Why is countermovement jump height greater than squat jump height? *Med. Sci. Sports Exerc.* **28**, 1402-1412.
Carrier, D. R., Heglund, N. C. and Earls, K. D. (1994). Variable gearing during locomotion in the human musculoskeletal system. *Science* **265**, 651-653.
Cronin, N. J., Carty, C. P., Barrett, R. S. and Lichtwark, G. (2011). Automatic tracking of medial gastrocnemius fascicle length during human locomotion. *J. Appl. Physiol.* **111**, 1491-1496.
Delp, S. L., Anderson, F. C., Arnold, A. S., Loan, P., Habib, A., John, C. T., Guendelman, E. and Thelen, D. G. (2007). OpenSim: open-source software to create and analyze dynamic Simulations of movement. *IEEE Trans. Biomed. Eng.* **54**, 1940-1950.
Farris, D. J. and Sawicki, G. S. (2012a). The mechanics and energetics of human walking and running: a joint level perspective. *J. R. Soc. Interface* **9**, 110-118.
Farris, D. J. and Sawicki, G. S. (2012b). Human medial gastrocnemius force-velocity behavior shifts with locomotion speed and gait. *Proc. Natl. Acad. Sci. USA* **109**, 977-982.
Farris, D. J., Robertson, B. D. and Sawicki, G. S. (2013). Elastic ankle exoskeletons reduce soleus muscle force but not work in human hopping. *J. Appl. Physiol.* **115**, 579-585.
Hof, A. L., Geelen, B. A. and Van den Berg, J. (1983). Calf muscle moment, work and efficiency in level walking; role of series elasticity. *J. Biomech.* **16**, 526-537.
Ishikawa, M., Komi, P. V., Grey, M. J., Lepola, V. and Bruggemann, G.-P. (2005). Muscle-tendon interaction and elastic energy usage in human walking. *J. Appl. Physiol.* **99**, 603-608.
Kurokawa, S., Fukunaga, T. and Fukashiro, S. (2001). Behaviour of fascicles and tendinous structures of human gastrocnemius during vertical jumping. *J. Appl. Physiol.* **90**, 1349-1358.
Kwah, L. K., Pinto, R. Z., Diong, J. and Herbert, R. D. (2013). Reliability and validity of ultrasound measurements of muscle fascicle length and pennation in humans: a systematic review. *J. Appl. Physiol.* **114**, 761-769.
Lichtwark, G. A. and Wilson, A. M. (2005). In vivo mechanical properties of the human Achilles tendon during one-legged hopping. *J. Exp. Biol.* **208**, 4715-4725.
Lichtwark, G. A. and Wilson, A. M. (2006). Interactions between the human gastrocnemius muscle and the Achilles tendon during incline, level and decline locomotion. *J. Exp. Biol.* **209**, 4379-4388.
Lichtwark, G. A. and Wilson, A. M. (2008). Optimal muscle fascicle length and tendon stiffness for maximising gastrocnemius efficiency during human walking and running. *J. Theor. Biol.* **252**, 662-673.
Plas, R. L., Degens, H., Meijer, J. P., de Wit, G. M., Philippens, I. H., Bobbert, M. F. and Jaspers, R. T. (2015). Muscle contractile properties as an explanation of the higher mean power output. *J. Exp. Biol* **218**, 2166-2173.
Rana, M., Hamarneh, G. and Wakeling, J. M. (2014). 3D curvature of muscle fascicles in triceps surae. *J. Appl. Physiol.* **117**, 1388-1397.
Roberts, T. J. and Azizi, E. (2011). Flexible mechanisms: the diverse roles of biological springs in vertebrate movement. *J. Exp. Biol.* **214**, 353-361.
Roberts, T. J. and Marsh, R. L. (2003). Probing the limits to muscle-powered accelerations: lessons from jumping. *J. Exp. Biol.* **206**, 2567-2580.
Schwartz, M. H. and Rozumalski, A. (2005). A new method for estimating joint parameters from motion data. *J. Biomech.* **38**, 107-116.